IEEE Access
Multidisciplinary ⋮ Rapid Review ⋮ Open Access Journal

Received 21 June 2024, accepted 8 July 2024, date of publication 11 July 2024, date of current version 31 July 2024.

Digital Object Identifier 10.1109/ACCESS.2024.3426936

RESEARCH ARTICLE

Electrical Behaviors During Rise and Fall of Pantograph of Electric Locomotive in Traction Power Supply System

LIKE PAN[1], TONG XING[1,2], ZHIQIANG YU[3], LIMING CHEN[1], CAIZHI YANG[1], AN JIN[4], XIAOYUN SUN[3], YUEHUA CUI[3], TAO FENG[3], XUDONG YI[3], JIANHUA CHEN[3], AND WENXIA YAN[3]

[1]Standards and Metrology Research Institute, China Academy of Railway Sciences Corporation Limited, Beijing 100081, China
[2]National Engineering Research Center of System Technology for High-Speed Railway and Urban Rail Transit, China Academy of Railway Sciences Corporation Ltd., Beijing 100081, China
[3]School of Electrical and Electronic Engineering, Shijiazhuang Tiedao University, Shijiazhuang 050043, China
[4]Railway Science and Technology Research and Development Center, China Academy of Railway Sciences Corporation Ltd., Beijing 100081, China

Corresponding author: Tong Xing (13810402255@163.com)

This work was supported in part by the Research Project of China Academy of Railway Sciences Group Company Ltd., under Grant 2022YJ151; in part by the Research Project of China State Railway Group Company Ltd., under Grant J2022J008; in part by the National Natural Science Foundation of China from the Chinese Ministry of Science and Technology under Grant U23A2068; in part by the Natural Science Foundation of Hebei Province of China under Grant E2021210022; in part by Hebei Provincial Collaborative Innovation Center of Transportation Power Grid Intelligent Integration Technology and Equipment, Shijiazhuang Tiedao University; in part by Hebei Key Laboratory for Electromagnetic Environment Effect and Information Processing under Grant ZZKT-202305; and in part by the Science and Technology Project of Hebei Education Department under Grant QN2020155.

ABSTRACT The off-line discharge between the pantograph and catenary (PAC) occurs frequently in the actual operation of an electric locomotive, which affects the quality of the received current and the service life of the pantograph. The current experiments on the off-line discharge between the PAC are mainly low-power ones and the models established are static. To study the electrical behaviors during the PAC relative motion under the actual working conditions, in this paper, the voltage and current of the contact wire (CW) during its motion are measured. And the electrical behaviors during the rise, fall and reciprocating motions of the pantograph are investigated by combining a finite element method (FEM) model based on the magnetohydrodynamics with the auto transformer (AT) traction network circuit and moving mesh method. It is found that the harmonic frequencies are mainly in the range of 0-30 MHz. The voltage distortion is more obvious during the fall of the pantograph. And the negative polarity spike pulse has a larger amplitude and occurs more frequently. The novelty of this paper lies in the experimental test with the high current and high power, as well as the systematic analysis of the electrical behaviors and multi-physical field evolution during the motion of the pantograph under the working conditions. Its contribution is to present an effective method to study the dynamic behaviors of the PAC. The research results can provide an important reference for the identification of the electrical characteristics of the PAC and the protection of the PAC equipment.

INDEX TERMS Electrical behaviors, pantograph and catenary (PAC), off-line discharge, auto transform (AT) traction network circuit, finite element method (FEM) model.

I. INTRODUCTION

Currently, most electric locomotives in the world use the sliding contact between the pantograph and catenary (PAC) to receive the electric energy [1], [2], [3]. The pantograph located on the top of the locomotive during its movement vibrates, leading to a short off-line discharge between the PAC. This makes many harmonic waves, greatly affecting the quality of the received current and deteriorating the rectification of the electrical drive system. Moreover, the arc due to the off-line discharge between the PAC causes the surfaces of the PAC to be abraded and oxidized, which reduces their working

The associate editor coordinating the review of this manuscript and approving it for publication was Diego Bellan.

lives and even affects the safety of the locomotive [4]. Therefore, it is necessary to study the electrical behaviors of electric locomotives during the vibration of the pantograph under the operating conditions (i.e. its rise and fall motion).

The electrical studies related to the PAC have focused on the experimental study [5], [6], [7], [8], [9], [10], off-line discharge of the PAC [11], [12], [13], [14], electromagnetic noise [15] and contact resistance [16]. In terms of experimental testing, in general, researchers built the low-power direct current (DC) [5], [6], [7] or alternating current (AC) [8], [9] devices in the laboratory to measure the voltage, current, and power consumption with small-current off-line discharging during the static or slow motion between the PAC. For modeling the arc caused by off-line discharge between the PAC, the Mayre model [17] and the Cassie model [18] are the classical analytical models as well as the Habedank model [19] developed based on the Cassie model. These models have fewer formulas, easy to integrate with the circuit network. And they are still used today. Kai et al. [20] considered the effect of the high-speed airflow on the arc power dissipation and improved the Mayr model to study the blown arc characteristics. Zhou et al. [21] established a dynamics model of a dual-pantographs-catenary system, analyzing their off-line states and trajectories. They introduced the Cassie model to study the discharge. With the development of the computer technology, a finite element method (FEM) model has become more and more common [13], [14]. Yu et al. [13] set up an arc model of the PAC off-line discharge in the urban rail based on the theory of magnetohydrodynamics. And they investigated the surface temperature of the pantograph with different materials and its distribution characteristics. Yu et al. [14] used hydrodynamics and Maxwell's equations to build the flow column model of the PAC off-line discharge, studying the process of the air ionization and the particle motion as well as the formation process of the impulse current. These FEM models have more formulas (especially the multi-field coupling model) but can visualize the distribution and changes of multiple physical quantities.

Recently, based on the polygonal contact principle, Yao et al. [22] established a collision dynamics model of the pantograph and investigated the contact force of the PAC. Gao et al. [23] proposed a temperature analytical model of the extended contact line when the pantograph rises and falls based on the thermo-power balance equations. And they studied the behaviors of the double sliding electrical contact of the PAC. Zhu et al. [24] used a low-power PAC experimental device to measure and analyze the parameters such as the stable ignition voltage and time during the rise of the pantograph. Jackson et al. [25] analyzed the variations of the velocity and pressure of the pantograph at different operating heights based on a three-dimensional fluid dynamics model. Song et al. [26] experimentally tested and simulated the contact force between pantograph and contact network at different speeds. They used a neural network algorithm to optimize the quality of the contact force at the four speeds. Kim et al. [27] described a three-dimensional unsteady turbulent flow around Faiveley CX pantograph by large-eddy simulations, exploring the aerodynamic force distributions on the structures of the pantograph. In summary, there are relatively few studies on the electrical characteristics when the pantograph rises or falls.

From the above, the researchers set up the low-power PAC experimental device to measure the electrical behaviors during their off-line. And the established arc models of the PAC off-line discharge were mainly used to study the situation when the PAC was relatively stationary. The experiment on the PAC off-line discharge with the high current and power, as well as the electrical behaviors and multi-physics field evolution during the motion or vibration of the pantograph under the working conditions, has not been solved. Therefore, in this paper,

1) A high-power high-speed railway PAC experimental device to measure the voltage and current at the large supply current (100 A) and high-speed motion (450 km/h) is employed and their time-domain and frequency characteristics are studied.

2) Based on the magnetohydrodynamics and combined with the auto transformer (AT) circuit and moving mesh method, a dynamic FEM model for realizing the motion of the pantograph of the electric locomotives under operating conditions is developed.

3) The electrical behaviors and multi-physical quantities during the rise, fall and reciprocating motion of the pantograph are researched, as well as the influence of the pantograph speed on them.

The structure of this paper is as follows: the section II briefly introduces the components of the PAC experimental device and its main parameters. The measured results are analyzed in the time domain and frequency domain; the section III establishes a dynamic model of the PAC and verifies it; the section IV discusses the electrical behaviors as well as the characteristics of the multi-physical fields during the rise, fall and reciprocating motion of the pantograph, also illustrating the effects of the speed of the pantograph on them; the section V is the conclusion. The research process of this paper is shown in Fig. 1.

This paper gives an effective method to research the dynamic behaviors of the PAC. The research results can provide an important reference for the identification of the electrical characteristics of the PAC and the protection of the PAC equipment.

II. EXPERIMENTAL DEVICE AND RESULTS

The main components of the PAC experimental device of high-speed rail are the mainframe, turntable with embedded the connect wire (CW), vibration table and pantograph installed on the vibration table (see Fig. 2a). Its main parameters are as follows: the rotational speed of the turntable ranging from 0-530 km/h, the leveling distance of ±350 mm, the power supply current of 0-1000 A, the vibration table

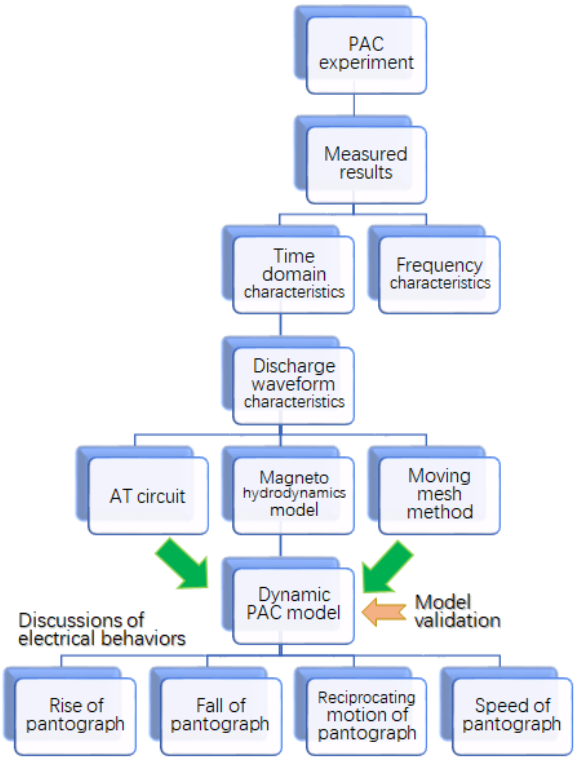

FIGURE 1. Block diagram of research process.

having a loading capacity of 180 kg, the acceleration of 0.75 m/s^2, and the vibration frequency of 0-30 Hz. The experimental device simulates the actual running state of a high-speed railway by setting the parameters of the rotational speed, the power supply current and the vibration frequency. The off-line discharge phenomenon occurs between the PAC (see Fig. 2b) [28]. The measurement circuit is in Fig. 2c.

High frequency harmonics appear in both the voltage and current (see Fig. 3). From the voltage curve, the complete shape of the arc can be clearly seen, including the initiation, ignition, and extinction stages. And the amplitude and frequency of the harmonics are larger in the initiation and extinction stages. In the ignition stage, which is the main stage of the discharge, the voltage and current are relatively more stable and fewer harmonics are generated. Also, the stable conductive channel is formed after the air between the PAC is pierced. And the discharge belongs to the balanced. The equivalent resistance of the plasma varies with some factors such as the plasma temperature and arc length. It increases the total resistance of the entire circuit, resulting in a slight decrease in the overall current, while causing the voltage between the PAC to be elevated. During the initiation and extinction stages, due to the drastic fluctuation of the current, the electric field around it also fluctuates significantly, which will generate the electromagnetic disturbance.

The FFT analyses of the above measurements show that the main frequency range of the current is 0-30 MHz, with higher amplitudes near the frequencies of 0.7, 1.5, 3.8-4, 5.5, 8.8, 11, and 21.8-23 MHz. The main frequency range of the harmonics of the current also less than 30 MHz, mainly distributed around the frequencies: 0-5, 5-10, 11-12, 15 and 20 MHz. The main range of the electric field spectrum is less than 60 MHz, mainly distributing near the frequencies of 0.3, 6.9-9.2, 4.7-10.6, 15.1, 29-34, 46, and 52 MHz. The fundamental components of the voltage and current are still their main components. And similar conclusions can be obtained in other cases of the CW currents and speeds.

III. DYNAMIC MODELING OF PAC

From the section II, the ignition stage occupies a larger part of the discharge process. To describe the physical processes accurately and highlight the stable discharge stage, a FEM model of the PAC is established based on the magnetohydrodynamics [13].

The pantograph mainly consists of the base frame, spring, arm, and slider (see Fig. 4a). The 2D geometrical model of the PAC consists of the CW, pantograph slider (PS) and air domain (see the left of Fig. 4b).

A. FUNDAMENTAL EQUATIONS

The basic equations of the magnetohydrodynamics include the Navier-Stokes equations and Maxwell's equations. And the magnetohydrodynamic vector equation is [13], [32]:

$$\frac{\partial \rho}{\partial t} + \rho \nabla \cdot \vec{v} = 0 \tag{1}$$

$$\rho \frac{\partial \vec{v}}{\partial t} = \vec{J} \times \vec{B} - \nabla P - \eta \nabla \times \nabla \times \vec{v} + \frac{4}{3}\eta \nabla \left(\nabla \cdot \vec{v} \right) \tag{2}$$

$$\rho \frac{dh}{dt} = \vec{J} \times \vec{E} + \nabla \cdot (k \nabla T) + Q - e_{tr} \tag{3}$$

(1)-(3) are the mass conservation, momentum conservation and energy conservation equation respectively, where ρ is the mass density, v is the velocity vector of the plasma, $J \times B$ is the vector of the electromagnetic force acting on the plasma, P is the pressure of the plasma, η is the viscosity coefficient, E is the electric field strength, k is the heat conduction coefficient, Q is the heat of reaction term, e_{tr} is the radiation term, $h = e + P/\rho$ is the enthalpy (per unit of mass), and T is the temperature. E, J and B are given by Maxwell's equations and Ohm's law.

For the temperature field, the temperature changes due to the interaction of the pantograph, as a discharge electrode, with the plasma. The equations are as [13] and [14]:

$$-n \cdot (-k \nabla T) = Q_b \tag{4}$$

$$Q_b = -J_{elec} \Phi_{eff} + J_{ion} V_{ion} \tag{5}$$

$$J_{elec} = \text{If} \left(|J \cdot n| > J_R, J_R, |J \cdot n| \right) \tag{6}$$

$$J_R = A_R T^2 \exp \left(-q \Phi_{eff} / k_B T \right) \tag{7}$$

$$J_{ion} = |J \cdot n| - J_{elec} \tag{8}$$

where J_{elec} is the electron current density, $\Phi_{eff} = 2.6$ V is the active function on the electrode surface, Jion is the ionic current density, $V_{\text{ion}} = 15.7$ V is the ionization potential, $A_R = 120$ A/(m^2·K^2) is the effective Richardson constant,

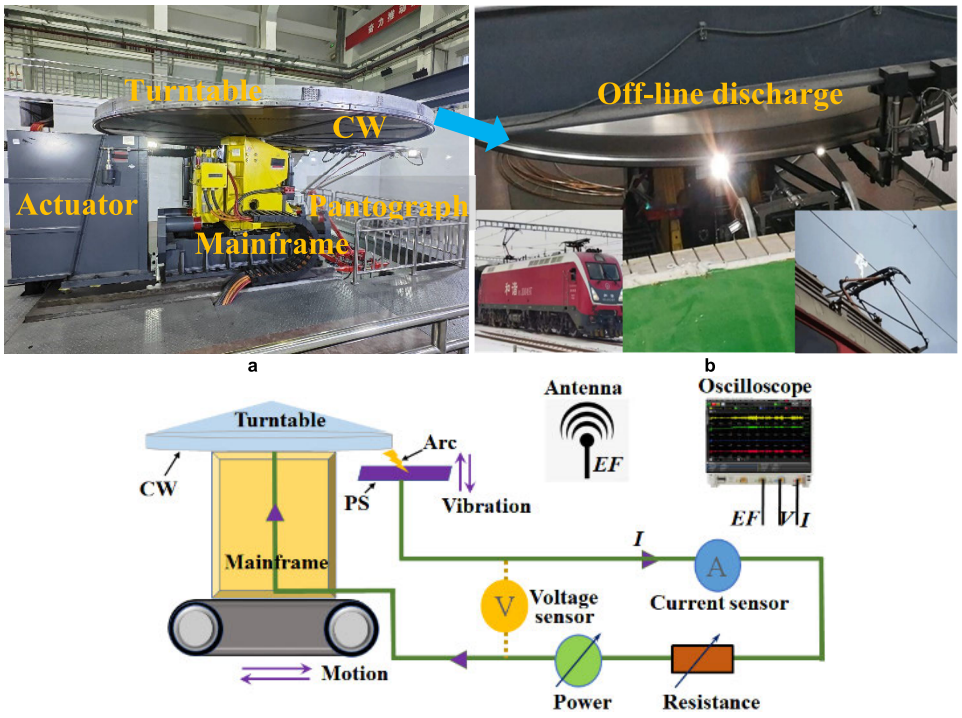

FIGURE 2. PAC experimental device: a. main components, b. off-line discharge (the left inset shows photo of locomotive and right inset is its pantograph) and c. measurement circuit diagram.

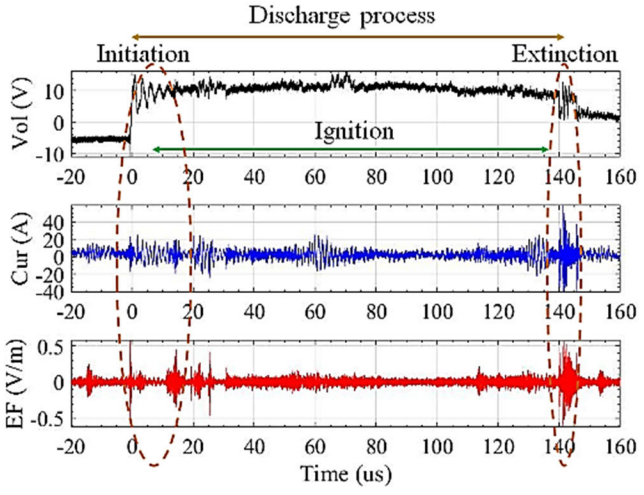

FIGURE 3. Current, voltage and electric field between PAC with RMS CW current of 100 A and speed of 450 km/h (Vol represents voltage, Cur for current and EF for electric field).

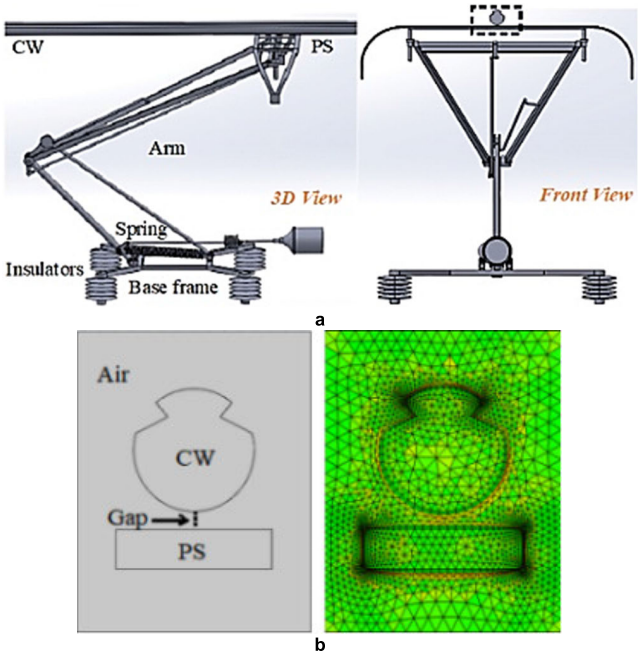

FIGURE 4. Pantograph-CW model: a. 3D geometrical model and b. 2D computational model and its mesh profile.

q is the electron charge, and $|J{\cdot}n|$ is the normal current density of the interface.

B. MOVING BOUNDARY CONDITIONS

For the fluid field, it can be regarded as the laminar flow. The surfaces of the CW and pantograph are set as the no-slip boundary. And the air boundary is set as the pressure exit boundary with one standard atmosphere. For the temperature field, the air is in the fluid state, the air boundary is set to be thermally insulated, i.e. $-n{\cdot}q{=}0$ (where q is for the conduction heat flux). And the initial temperature of the whole computational region is room temperature (293.15 K).

For the electric field, the whole computational region follows the law of the conservation. And the air boundary is

set to be electrically insulating i.e. $n \cdot J = 0$. Since the cathode emits electrons to the anode, the lower end of the CW is set to be the input boundary condition of the current density [26]. For the magnetic field, the whole computational region follows the Ampere's law, and the air boundary is set to be magnetically insulated. The moving mesh method is used to realize the motion of pantograph. (see the right of Fig. 4b).

C. MODEL VALIDATION

Based on the above magnetohydrodynamic equations and boundary conditions, the FEM software [13], [30], [31] is used for modeling and the calculated results with the measured are compared [32] (see Fig. 5).

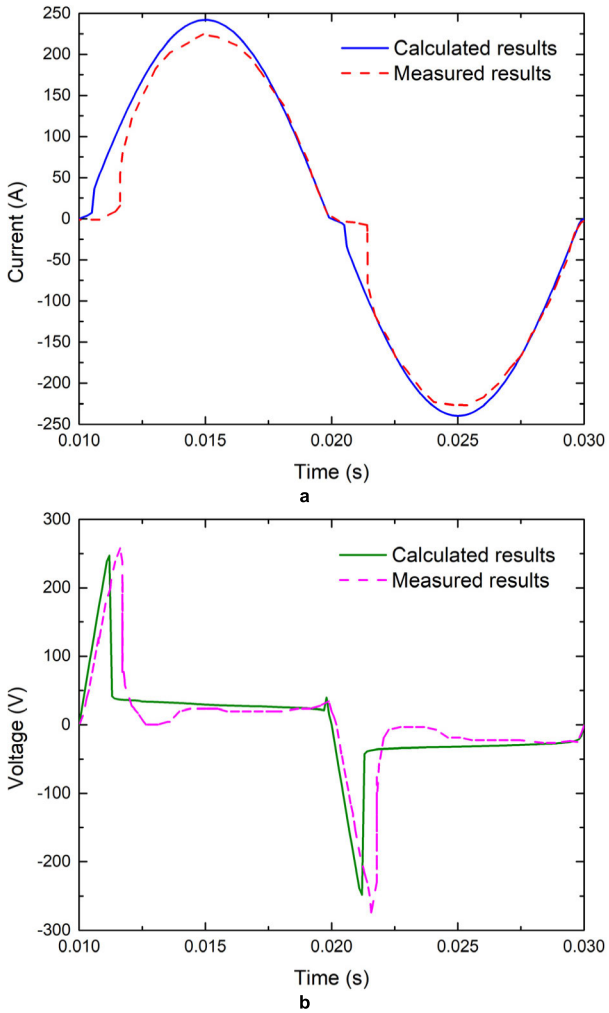

FIGURE 5. Comparison of calculation results of PAC off-line discharge with measured results [32]: a. voltage and b. current.

The current overall presents a sinusoidal waveform (see Fig. 5a). When the pantograph is separated from the CW, the discharge happens and the arc ignites. It is extinguished near the zero point and then ignites again. That is, there is a transient zero-rest phenomenon. The distortion of the voltage is larger. In the early stage of the discharge there is a sudden increase on the voltage waveform (see Fig. 5b), when the voltage acts on the air between the PAC. While the air is punctured, its equivalent resistance decreases rapidly and the voltage decreases instantaneously. During arc re-ignition, the voltage exhibits the same process as the ignition. A comparison shows that the maximum error between the calculated and measured results is 4.3% for the voltage and 4.0% for the current. These show that the model developed in this paper is correct and can be used to study and analyze the dynamic electrical behaviors of the PAC when the pantograph rises or falls.

IV. RESULTS AND DISCUSSION

The established FEM model of the PAC with the AT traction circuit is simulated jointly. And the electrical behaviors and multi-physical field behaviors during the rise, fall and reciprocating motions of the pantograph are discussed, as well as the influence of the speed on them.

In Fig. 6, the parameters of the AC voltage source are 27.5 kV, 50 Hz, Rs=0.2496 Ω, Ls=12.64 mH. And the distributed impedances to ground are Cj=0.69 pF, Rj=0.01 Ω and Lj=1.0278 × 10^{-4} H, respectively. The equivalent impedances of the car body are Rt=0.063 Ω, Lt=0.223 mH and Ct=4.25 μF [33], respectively. The voltage between the pantograph and ground, as well as the current flowing through the pantograph, is sinusoidal when the PAC are in good contact. Their amplitudes are 27.5 kV and 202.74 A, respectively. According to the actual situation of the PAC, in the following simulation, the speed of the pantograph is 2 cm/s for 0.1 s. The initial gap between the PAC is 2.5 mm.

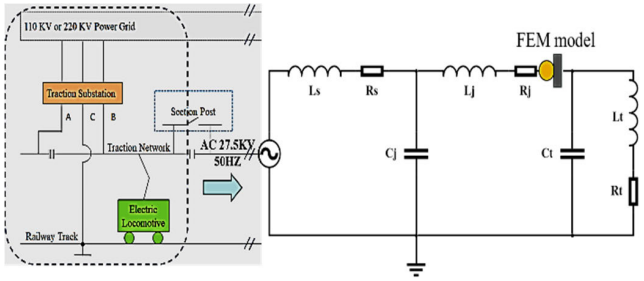

FIGURE 6. AT traction network circuit coupled FEM model.

A. RISE OF PANTOGRAPH

The current is sinusoidal during the rise of the pantograph, with the amplitude of 202 A (see Fig. 7). Compared to the current, the value of the voltage between the PAC is smaller. However, it shows the spike pulses, with a maximum spike value of −185 V. The maximum distortion ratio ((sharp peak-normal peak)/normal peak) is (−185+25)/(−25)=6.4 and the average distortion ratio (∑ distortion ratios/∑number of normal peaks) is 1.46. When t>0.4 s, the spike pulse disappears (the spike frequency is 5/10=0.5) and the voltage amplitude gradually becomes smaller. The reason for this is believed that with the decrease of the gap between the PAC,

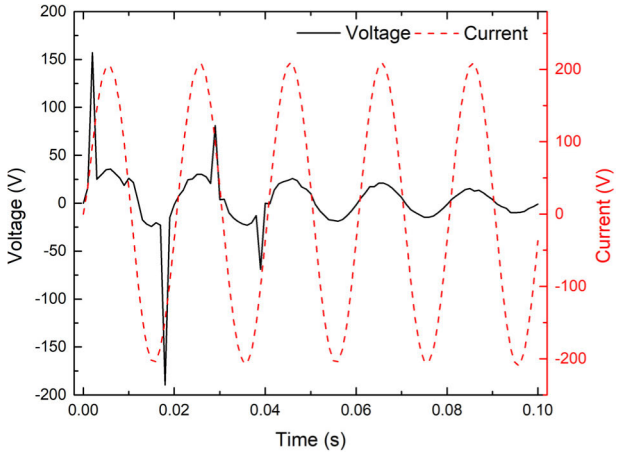

FIGURE 7. Voltage and current during rise of pantograph.

While the current flowing through is almost constant, the voltage between the PAC gradually decreases. And the pulse appears near the voltage peak where the gradient change is larger. At this time the plasma is in violent motion, causing its resistance to a sudden change. The reason that current does not contain distorted harmonics is that the corona discharge (i.e. the air ionization process) is not considered in the model [14] and the small arc resistance makes the impedance of the entire circuit not change significantly. So the overall current waveform does not change. This agrees with the experimental results generally [29].

The area of high temperature is the arc region (see the first row of Fig. 8). The highest temperature area is located at the center of the gap. As the pantograph rises, the arc region narrows. The temperature on the bottom of the CW shows a symmetrical distribution with a high center and two low ends. From 0.01 s to 0.1 s, the temperature at the midpoint

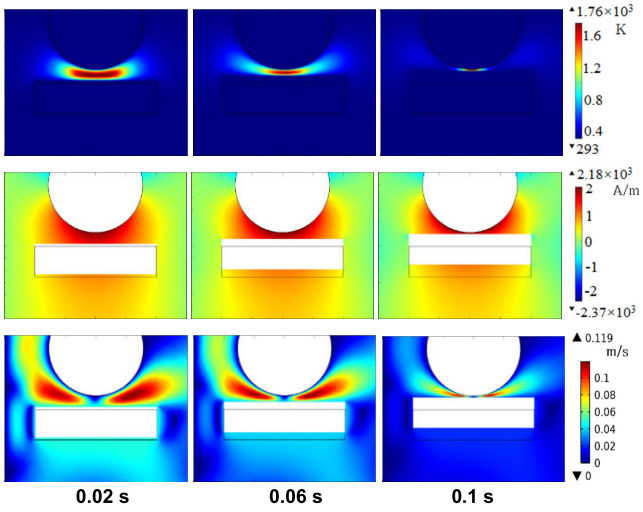

FIGURE 8. Dynamic distributions of temperature, electromagnetic and air flow field between PAC during rise of pantograph (the times for the three columns are 0.02, 0.06 and 0.1 s, respectively).

of the bottom of the CW increased by 7 K, indicating the accumulation effect of the temperature.

The magnetic field strength is greater in the region where the CW is in contact with the arc. And its value increases gradually with the reduction of the gap, with the maximum value of 2.18×10^3 A/m (see the second of Fig. 8). The distributions of the velocity field are related to the shape of the CW as well as the size of the gap, wrapping along the bottom of the CW and spreading out to the sides (see the last of Fig. 8). The air on both sides of the bottom of the CW has the higher velocity and lower velocity than in other regions.

B. FALL OF PANTOGRAPH

During the fall of the pantograph, the current is still a sinusoidal wave. While the upper and lower half waves of the voltage both have spike pulses. And the amplitude of the negative pulse is larger than that of the positive (see Fig. 9). When $t >= 0.05$ s, the average value of the pulses is larger than that when $t < 0.05$ s. This is since the plasma motion is more violent when the gap increases. In general, compared with the rise of the pantograph, when it falls, the spike pulse appears with increased frequency and larger amplitude. The larger the gap, the larger the resistance of the plasma and the spike.

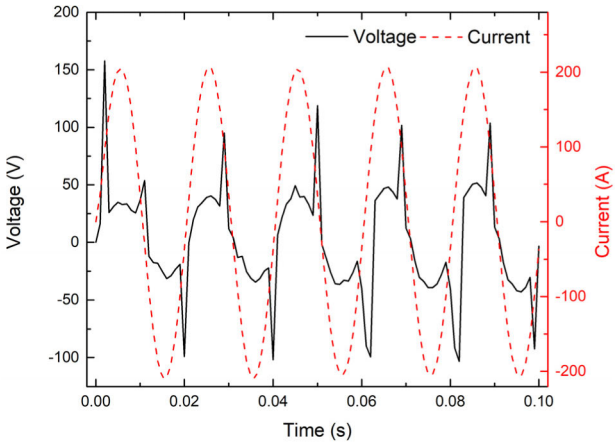

FIGURE 9. Voltage and current during fall of pantograph.

The temperature is lower than that when the pantograph rises (see Fig. 10). This is due to the increase in the gap, which leads to the intensification of air convection and thus facilitates heat dissipation. The discharge arc (red area) gradually becomes longer and wider. And the highest temperature is around the arc column, gradually decreasing along its radial direction. The magnetic field decreases gradually along the negative direction of the z axis. And its maximum value is still 2.07×10^3A/m. This is because the gap increases with the fall of the pantograph so that the arc is stretched. So, the current density decreases resulting in a decrease in the magnetic field. In this process the air flow velocity decreases, with a maximum of 0.04 m/s.

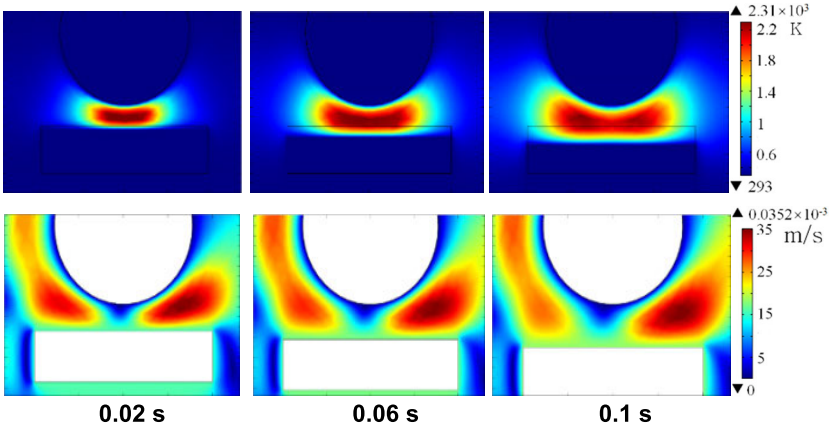

FIGURE 10. Dynamic distributions of temperature and air flow field between PAC during fall of pantograph.

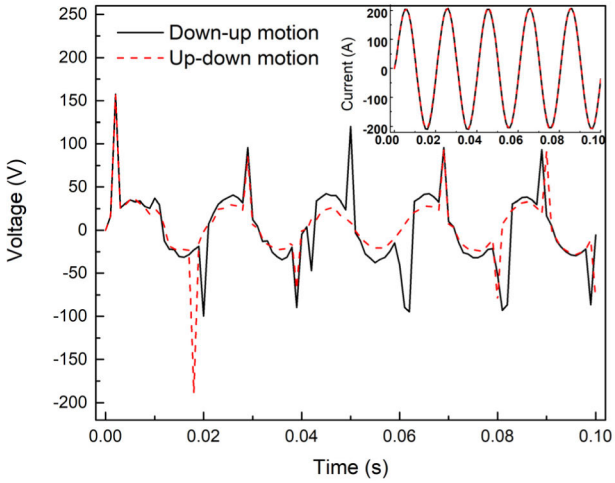

FIGURE 11. Voltage and current during reciprocating motion of pantograph.

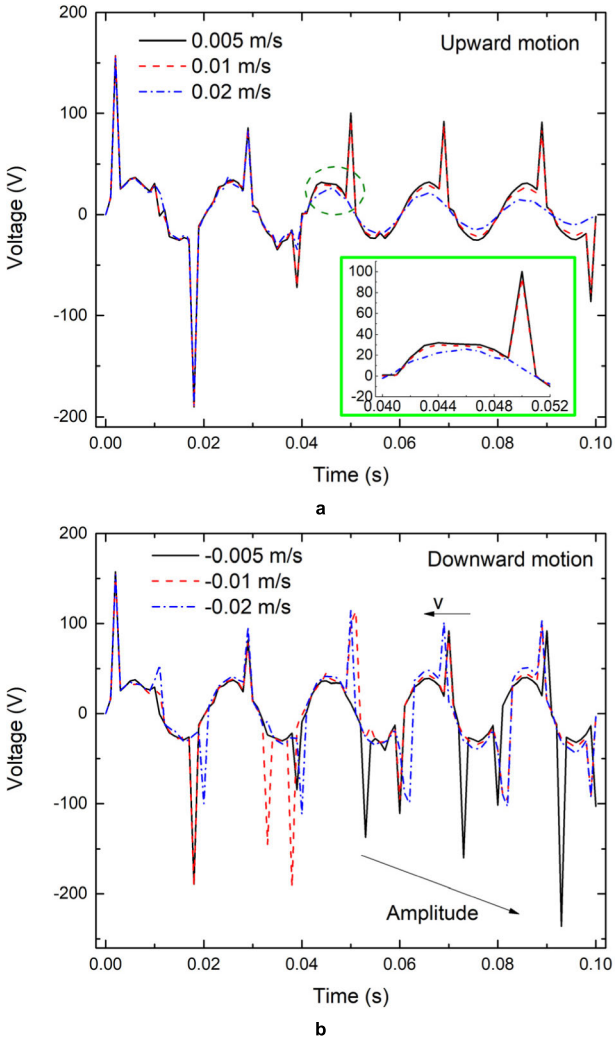

FIGURE 12. Voltage at different speeds of pantograph: a. upward and b. downward motion.

C. RECIPROCATING MOTION OF PANTOGRAPH

To study the electrical characteristics during the vibration of the pantograph, its reciprocating process including the down-up motion and up-down motion is simulated, of which the first stage of the motion time is 0.05 s and the second is 0.05 s).

The variations of the voltage are different in the two stages (see Fig. 11). In the first stage (0-0.05 s), compared with the down-up motion, the voltage with the up-down motion appeared a larger negative spike pulse (the maximum distortion ratio is 6.52). And it appeared earlier, less frequently. The waveform gradually flattened. In the second stage (0.05 s-0.1 s), the amplitude of the spike pulse with the up-down motion is lower than that with the down-up motion. And its frequency is still less. Overall, the spike frequency for the up-down motion is 0.8 and its average distortion ratio is 2.1, while the spike frequency for the down-up motion is 1.2 and its average distortion ratio is 3.1. So the degree of voltage distortion with the up-down motion is lower than that with the down-up motion. That is, the larger the range of gap variation, the more violent the plasma motion and the more unstable the electrical behaviors.

D. INFLUENCE OF SPEED OF PANTOGRAPH ON ELECTRICAL BEHAVIORS

The speed has no effect on the current but has a greater effect on the voltage (see Fig. 12). As the pantograph rises, the voltage amplitude and spike values decrease gradually with the increase of the speed, as well as the number of the pulse (see Fig. 12a). In particular, when $v = 0.02$ m/s, the spike pulse no longer occurs at $t = 0.05$ s. This indicates that at this time the gap is very small and the plasma is already very stable. For the fall of the pantograph at different speeds, during the positive voltage, the faster the speed, the earlier the moment of the spike pulse appears (see Fig. 12b). In the negative voltage, the slower the speed, the larger the pulse amplitude. And it keeps increasing with the gap, also indicating the more violent motion of the plasma. In conclusion, the degree of the voltage distortion is greater with the fall of the pantograph than that with its rise.

The results discussed above are obtained for the given typical parameters and circuit structure. When some parameters or the circuit structure change, these results can still be used as a basis for the qualitative analysis. For example, when the supply voltage of the AT traction network decreases, the current amplitude decreases as well as that of the spike pulse in the voltage. And the other electrical behaviors remain unchanged; when the initial gap between the PAC increases, the amplitude of the spike pulse increases and the current remains unchanged; when the crosswind (i.e., the increase in the air flow velocity) occurs near the PAC, the amplitude of the spike pulse and its frequency increase, but the arc temperature decreases.

V. CONCLUSION

In this paper, the voltage and current during the relative high-speed operation between the PAC are measured by the high-power experimental equipment. Then a dynamic model of the PAC based on the magnetohydrodynamics is established and verified. The model also applies the moving grid technology and coupled the actual AT traction network circuit. The main conclusions are as follows:

1) The high-frequency oscillations occur in the arc initiation and extinction stages, smoother in the ignition stage. The main frequency ranges of the voltage and current are 0-30 MHz.

2) When the pantograph rises or falls, the voltage has the spike pulse at the place where the gradient of the curve is larger near the peak. For the fall of pantograph, the pulse amplitude and frequency are larger than that with its rise. When the pantograph reciprocates, in the downward motion stage, the voltage appears to have a larger value of the spike pulse and more frequent. That is, the larger the range of the gap, the more violent the motion of the plasma, the more unstable the electrical characteristics.

3) As the pantograph rises, the amplitudes of the voltage and the pulse decrease gradually with increasing speed, as well as the number of the pulse. When the pantograph falls, during the positive voltage, the faster the speed, the earlier the moment of the spike pulse appears. While during the negative voltage, the slower the speed, the larger the pulse amplitude.

The modeling approach proposed in this paper could be applied to the digital simulation of high-current discharge experiments with a continuously varying discharge gap. The discharge frequencies obtained from the experiment can be used in the field of the electromagnetic protection and electromagnetic interference of high-speed railways. The limitation of this modeling approach is that only the equilibrium plasma discharge in the ignition stage is considered but the corona discharge process is not included. In the next step, the corona discharge features will be added to the model to make it more complete.

Conceptualization, Like Pan; Project Administration, Tong Xing and Liming Chen; Methodology, Zhiqiang Yu; Software, Caizhi Yang and An Jin; Writing–Review & Editing, Xiaoyun Sun; Data Curation, Yuehua Cui and Tao Feng; Investigation, Xudong Yi; Validation, Jianhua Chen and Wenxia Yan.

ACKNOWLEDGMENT

The authors would like to sincerely thank the anonymous reviewer for his/her opinions to improve the quality of the article.

REFERENCES

[1] S. Rusu-Anghel, S. S. Mezinescu, and I. C. Lihaciu, "Experimental stand and researches on pantograph-catenary contact force control using chaos theory," *J. Phys., Conf. Ser.*, vol. 1781, no. 1, Feb. 2021, Art. no. 012029, doi: 10.1088/1742-6596/1781/1/012029.

[2] V. Y. Ushakov, A. V. Mytnikov, and I. U. Rakhmonov, "Characteristics of the main elements of electric power systems," in *High-Voltage Equipment of Power Systems: Design, Principles of Operation, Testing, Monitoring and Diagnostics*. Cham, Switzerland: Springer, 2023, pp. 17–80, doi: 10.1007/978-3-031-38252-9.

[3] Z. Deng, W. Zhang, J. Zheng, B. Wang, Y. Ren, X. Zheng, and J. Zhang, "A high-temperature superconducting maglev-evacuated tube transport (HTS maglev-ETT) test system," *IEEE Trans. Appl. Supercond.*, vol. 27, no. 6, pp. 1–8, Sep. 2017, doi: 10.1109/TASC.2017.2716842.

[4] Y. Yao, N. Zhou, D. Zou, G. Mei, and W. Zhang, "Collision dynamics analysis of lifting the pantograph," *Proc. Inst. Mech. Engineers, F, J. Rail Rapid Transit*, vol. 235, no. 4, pp. 450–462, Apr. 2021, doi: 10.1177/0954409720943397.

[5] S. Midya, D. Bormann, T. Schutte, and R. Thottappillil, "Pantograph arcing in electrified railways—Mechanism and influence of various parameters—Part I: With DC traction power supply," *IEEE Trans. Power Del.*, vol. 24, no. 4, pp. 1931–1939, Oct. 2009, doi: 10.1109/TPWRD.2009.2021035.

[6] T. Xin, C. Roberts, P. Weston, and E. Stewart, "Condition monitoring of railway pantographs to achieve fault detection and fault diagnosis," *Proc. Inst. Mech. Engineers, F, J. Rail Rapid Transit*, vol. 234, no. 3, pp. 289–300, Mar. 2020, doi: 10.1177/0954409718800567.

[7] P. Nåvik, S. Derosa, and A. Rønnquist, "On the use of experimental modal analysis for system identification of a railway pantograph," *Int. J. Rail Transp.*, vol. 9, no. 2, pp. 132–143, Mar. 2021, doi: 10.1080/23248378.2020.1786743.

[8] S. Midya, D. Bormann, T. Schutte, and R. Thottappillil, "Pantograph arcing in electrified railways—Mechanism and influence of various parameters—Part II: With AC traction power supply," *IEEE Trans. Power Del.*, vol. 24, no. 4, pp. 1940–1950, Oct. 2009, doi: 10.1109/TPWRD.2009.2021036.

[9] A. Hu and P. Paoletti, "A novel control architecture for marginally stable dynamically substructured systems," *Mech. Syst. Signal Process.*, vol. 143, Sep. 2020, Art. no. 106834.

[10] L. Ma, Y. Wen, A. Marvin, E. Karadimou, R. Armstrong, and H. Cao, "A novel method for calculating the radiated disturbance from pantograph arcing in high-speed railway," *IEEE Trans. Veh. Technol.*, vol. 66, no. 10, pp. 8734–8745, Oct. 2017, doi: 10.1109/TVT.2017.2704611.

[11] E. Schade and D. Leonidovich Shmelev, "Numerical simulation of high-current vacuum arcs with an external axial magnetic field," *IEEE Trans. Plasma Sci.*, vol. 31, no. 5, pp. 890–901, Oct. 2003, doi: 10.1109/TPS.2003.818436.

[12] W. Xie, G. Wu, W. Wei, Z. Yang, and G. Gao, "Research on characteristics of the pantograph arc under the action of magnetic field," in *Proc. IEEE Int. Conf. High Voltage Eng. Appl. (ICHVE)*, Beijing, China, Sep. 2020, pp. 1–4, doi: 10.1109/ICHVE49031.2020.9279511.

[13] X. Yu, M. Song, and Z. Wang, "Simulation study on surface temperature distribution of collector strip material under pantograph-catenary arc of urban rail," *IEEE Access*, vol. 11, pp. 68358–68365, 2023, doi: 10.1109/ACCESS.2023.3292277.

[14] Z. Yu, C. Zhang, X. Sun, T. Xing, L. Chen, and S. Liu, "Measurement and analysis of electrical behaviors of offline discharge between high-speed contact wire and pantograph of locomotive," *IEEE Trans. Instrum. Meas.*, vol. 72, pp. 1–12, 2023, doi: 10.1109/TIM.2022.3229718.

[15] Y. Yudhistira, Y. Yoppy, E. Trivida, T. A. W. Wijanarko, H. W. Nugroho, and D. Mandaris, "Electromagnetic interference measurement for axle counters light rapid transit railway in Indonesia," *Int. J. Electr. Comput. Eng. (IJECE)*, vol. 12, no. 5, p. 4632, Oct. 2022.

[16] H. Zhou, F. Duan, Z. Liu, L. Chen, Y. Song, and Y. Zhang, "Study on electric spark discharge between pantograph and catenary in electrified railway," *IET Electr. Syst. Transp.*, vol. 12, no. 2, pp. 128–142, Mar. 2022, doi: 10.1049/els2.12043.

[17] O. Mayr, "Beiträge zur theorie Des.statischen und des dynamischen Lichtbogens," *Archiv für Elektrotechnik*, vol. 37, no. 12, pp. 588–608, Dec. 1943, doi: 10.1007/bf02084317.

[18] A. M. Cassie, "Theorie nouvelle des arcs de rupture et de la rigidité des Circuits," *Cigre Rep.*, vol. 102, pp. 588–608, 1939.

[19] U. Habedank, "Application of a new arc model for the evaluation of short-circuit breaking tests," *IEEE Trans. Power Del.*, vol. 8, no. 4, pp. 1921–1925, Oct. 1993, doi: 10.1109/61.248303.

[20] Q. Kai, L. Wenzheng, Z. Jian, W. Tianyu, and G. Zhaofeng, "Simulation analysis of pantograph-catenary arc based on improved Mayr model," *Railway Standard Des.*, vol. 62, pp. 138–142, May 2018, doi: 10.13238/j.issn.1004-2954.201705230002.

[21] H. Zhou, Z. Liu, J. Xiong, and F. Duan, "Characteristic analysis of pantograph–catenary detachment arc based on double-pantograph–catenary dynamics in electrified railways," *IET Electr. Syst. Transp.*, vol. 12, no. 4, pp. 238–250, Aug. 2022, doi: 10.1049/els2.12049.

[22] Y. Yao, N. Zhou, G. Mei, and W. Zhang, "Analysis of collision dynamics of lifting the pantograph during vehicle operation," *Proc. Inst. Mech. Engineers, F, J. Rail Rapid Transit*, vol. 236, no. 7, pp. 793–802, Aug. 2022, doi: 10.1177/09544097211042690.

[23] S. Gao, Y. Wang, Z. Liu, X. Mu, K. Huang, and X. Song, "Thermal distribution modeling and experimental verification of contact wire considering the lifting or dropping pantograph in electrified railway," *IEEE Trans. Transport. Electrific.*, vol. 2, no. 2, pp. 256–265, Jun. 2016, doi: 10.1109/TTE.2016.2558841.

[24] G. Zhu, G. Gao, G. Wu, Z. Gu, J. Wu, and J. Hao, "Modeling pantograph-catenary arcing," *Proc. Inst. Mech. Eng. F J. Rail Rapid Transit*, vol. 230, pp. 1687–1697, Aug. 2016, doi: 10.1177/0954409715607906.

[25] F. F. Jackson, R. Mishra, J. M. Rebelo, J. Santos, P. Antunes, J. Pombo, H. Magalhães, L. Wills, and M. Askill, "Modelling dynamic pantograph loads with combined numerical analysis," *Railway Eng. Sci.*, vol. 32, no. 1, pp. 81–94, Mar. 2024, doi: 10.1007/s40534-023-00318-0.

[26] Y. Song, X. Lu, Y. Yin, Y. Liu, and Z. Liu, "Optimization of railway pantograph-catenary systems for over 350 km/h based on an experimentally validated model," *IEEE Trans. Ind. Informat.*, vol. 20, no. 5, pp. 7654–7664, May 2024, doi: 10.1109/TII.2024.3361485.

[27] S. J. Kim, H. Kwon, and J. Ahn, "Aerodynamic performance of a pantograph cover for high-speed train," *J. Mech. Sci. Technol.*, vol. 37, no. 9, pp. 4681–4693, Jul. 2023, doi: 10.1007/s12206-023-0823-9.

[28] X. Yan, C. Cheng, J. Hu, Y. Bai, and W. Zhang, "Design and implementation of a novel high-frequency current transformer for partial discharge measurements," *IEICE Electron. Exp.*, vol. 20, no. 23, Dec. 2023, Art. no. 20230450, doi: 10.1587/elex.20.20230450.

[29] K. C. Hsu, K. Etemadi, and E. Pfender, "Study of the free-burning high-intensity argon arc," *J. Appl. Phys.*, vol. 54, no. 3, pp. 1293–1301, Mar. 1983, doi: 10.1063/1.332195.

[30] Z. Cai, X. Zhang, and H. Cheng, "Evaluation of DC-subway stray current corrosion with integrated multi-physical modeling and electrochemical analysis," *IEEE Access*, vol. 7, pp. 168404–168411, 2019, doi: 10.1109/ACCESS.2019.2953960.

[31] J. F. D. Santos, B. K. Tshoombe, L. H. B. Santos, R. C. F. Araújo, A. R. A. Manito, W. S. Fonseca, and M. O. Silva, "Digital twin-based monitoring system of induction motors using IoT sensors and thermo-magnetic finite element analysis," *IEEE Access*, vol. 11, pp. 1682–1693, 2023, doi: 10.1109/ACCESS.2022.3232063.

[32] Z. Guangya, W. Guangning, H. Weifeng, G. Guoqiang, and L. Xianrui, "Simulation and analysis of the static lifting and lowering pantograph's steady-state arc characteristics of high-speed trains," *J. China Railway Soc.*, vol. 38, pp. 42–47, Feb. 2016.

[33] L. Tian and H. Li, "Simulation of electric arc characteristics based on MATLAB/simulink," *IOP Conf. Ser., Mater. Sci. Eng.*, vol. 452, Aug. 2018, Art. no. 042080, doi: 10.1088/1757-899X/452/4/042080.

LIKE PAN was born in Shaanxi, China, in 1986. He received the Ph.D. degree in vehicle operation engineering from Beijing Jiaotong University, Beijing, China, in 2017. His research interests include electrified railway traction power supply technology and pantograph-catenary coupling technology.

TONG XING was born in Beijing, China, in 1983. He received the master's degree in power systems and automation from China Academy of Railway Sciences, Beijing, China, in 2008. His research interests include pantograph-catenary coupling technology and collector shoe-contact rail coupling technology.

ZHIQIANG YU was born in Hebei, China, in 1977. He received the Ph.D. degree in theory and new technology of electrical engineering from the Institute of Electrical Engineering, Chinese Academy of Sciences, Beijing, China, in 2016. His research interests include electromagnetic, thermal, and other multiphysics coupled simulation, electromagnetic compatibility, principle of the superconducting magnetic levitation, and design of the flywheel energy storage systems.

LIMING CHEN was born in Hebei, China, in 1979. He received the M.S. degree in engineering mechanics from Beijing University of Technology, Beijing, China, in 2006. His research interests include electrified railway traction power supply technology and pantograph-catenary coupling technology.

CAIZHI YANG was born in Heilongjiang, China, in 1988. He received the bachelor's degree in mechanical engineering from Beijing University of Technology, Beijing, China, in 2013. His research interests include electrified railway traction power supply technology and pantograph-catenary coupling technology.

AN JIN was born in Hebei, China, in 1995. She received the M.S. degree in electrical engineering from Shijiazhuang Railway University, in 2020. Since 2020, she has been an Assistant Researcher with the Railway Science and Technology Research and Development Center, China Academy of Railway Sciences Corporation Ltd., and the National Engineering Research Center of System Technology for High-Speed Railway and Urban Rail Transit. She engaged in research related to traction power supply technology for rail transit.

XIAOYUN SUN was born in Hebei, China, in 1971. She received the Ph.D. degree in theory and new technology of electrical engineering from Xi'an Jiaotong University, Xi'an, China, in 2000. Her current research interests include electromagnetic compatibility and nondestructive testing.

YUEHUA CUI was born in Shijiazhuang, China, in 1978. He received the M.S. degree in power electronics and power transmission from Shijiazhuang Railway Institute, Shijiazhuang, in 2010. His research interests include electrical control and power supply and distribution technology.

TAO FENG was born in Hebei, China, in 1979. He received the M.S. degree in power electronics and power transmission from Shijiazhuang Railway Institute, Shijiazhuang, China, in 2010. His research interests include power electronics technology and high voltage technology.

XUDONG YI was born in Hebei, China, in 1998. He is currently pursuing the M.S. degree in electrical engineering with Shijiazhuang Tiedao University. His research interests include basic research on pantograph-net electrical contacts, and electromagnetic-thermal distribution studies of pantograph-catenary transient and steady-state contacts.

JIANHUA CHEN was born in Hebei, China, in 1997. He is currently pursuing the M.S. degree in electrical engineering with Shijiazhuang Tiedao University. His research interest includes the electrical contact properties of urban rail trains.

WENXIA YAN was born in Hebei, China, in 1998. She is currently pursuing the M.S. degree in electrical engineering with Shijiazhuang Tiedao University. Her research interests include the temperature distribution of boot-rail contact and its current-carrying stability.